Iacovelli C. et al., ***Cortical Network Topological Modifications Underlie Clinical Evolution in the Acute Phase of Ischemic Stroke***, in *Neurorehabil Neural Repair*. 39 (2025) 11, pp. 920-930.

Cortical Network Topological Modifications Underlie Clinical Evolution in the Acute Phase of Ischemic Stroke

Chiara Iacovelli, MSc, PhD[1*], Giuseppe Reale, MD, PhD[2*], Giulia Baldazzi, MSc, PhD[3], Danilo Pani, MSc, PhD[3], Aurelia Zauli, MD[4], Marco Moci, MD[2,5], Paolo Manganotti, MD, PhD[6], Lucio Marinelli, MD, PhD[7], Simona Sacco, MD[8], Giovanni Furlanis, MD[6], Miloš Ajčević, MSc, PhD[6], Silvia Giovannini, MD, PhD[9,10], Simona Crosetti, BSc[11], Matteo Grazzini, MD[12], Marta Garbuglia, MD[5], and Pietro Caliandro, MD, PhD[4]

Abstract

Background. Following stroke, brain networks can be described by strength of local connections (clustering coefficient [*Cw*]) and strength of global interconnections (path length [*Lw*]) between nodes, and their balance (Small-worldness [*Sw*]). *Objective*. To identify electroencephalography (EEG) networks predicting clinical evolution in stroke through a multicenter cross-sectional study. *Methods*. We consecutively recruited 87 anterior circulation ischemic stroke patients. We obtained resting-state EEG (31 electrodes, 10-10 system) within 24 hours from stroke (*T0*) and at discharge from stroke unit (4–10 days after stroke; *T1*). EEG data were elaborated with EEGLAB and Lagged Linear Coherence among cortical sources of EEG signals was analyzed using eLORETA. We performed a multiple linear regression with National Institutes of Health Stroke Scale (NIHSS) at *T0* and *T1* as dependent variables and *Cw*, *Lw*, and *Sw* of delta, theta, and alpha networks as independent variables. *Results*. We found a negative association between alpha1 *Sw* and NIHSS at *T0* ($\beta = -.232$, $P = .04$) meaning that the lower is alpha efficiency the higher is clinical severity and a positive association between delta *Sw* and NIHSS at *T1* ($\beta = .423$, $P < .001$) meaning that the higher is delta efficiency the higher is clinical severity. We found positive association between delta *Sw* at *T0* and NIHSS at *T1* ($\beta = .259$, $P = .02$), meaning that the higher is delta efficiency in the hyperacute phase the higher is clinical severity at *T1*. *Conclusions*. A higher delta *Sw* within 24 hours after stroke is associated to higher NIHSS within 10 days. Delta brain network rearrangement in the hyperacute phase is a potential neurophysiological measure to be integrated in multi-modal prognostic models.

Keywords

brain networks, stroke, EEG, recovery, prognosis, cortical connectivity

Introduction

Following an ischemic stroke, brain connectivity can experience complex changes.[1] Several studies employing different techniques, such as functional magnetic resonance imaging (fMRI) and electroencephalography (EEG), have explored the relationship between connectivity changes and clinical features, highlighting that specific connectivity rearrangements underlie specific neurological deficits and global clinical severity.[2] While fMRI provides excellent spatial resolution, resting-state EEG offers a direct measure of neuronal oscillatory activity and network dynamics with high temporal resolution, making it a valuable and feasible tool for bedside assessment, especially in the acute phase of stroke. Some studies have examined connectivity modifications over the period from stroke onset to the chronic phase, revealing that these changes predominantly occur within the first 3 months post-stroke and tend to diminish in the chronic phase.[3-11] In particular, longitudinal EEG studies have demonstrated that connectivity rearrangements and alterations in spectral power over time are closely associated with variations in neurological impairment.[3,6,12] However, to our knowledge, while some EEG studies have investigated spectral characteristics and symmetry indices as predictors of motor or global neurological recovery,[13] a detailed exploration of the evolution of resting-state EEG network topological characteristics in the very first days after stroke, and their direct predictive value for early clinical evolution, remains less defined, especially concerning the hyperacute phase. The utility of resting-state

EEG as a biomarker in stroke recovery is increasingly recognized. For instance, specific EEG spectral power, namely delta/alpha ratio and Brain Symmetry Index, have shown promise in predicting upper limb motor impairment and global neurological recovery longitudinally.[12,13] Moreover, in chronic stroke, alterations in EEG rhythms and network metrics, such as increased low-frequency activity and changes in node strength, have been correlated with motor functions.[14] These studies emphasize the sensitivity of EEG to stroke-induced neurophysiological alterations. Building upon this, investigating the graph theory-based topological properties of EEG networks in the earliest phases of stroke could offer deeper and complementary insights into the immediate brain response to injury and its implications for subsequent clinical trajectory. In a previous study we primarily explored whether EEG-based brain resting-state networks change in the acute ischemic stroke phase compared to healthy subjects. We found that in this phase brain networks experience complex changes in a frequency-dependent modality.[15] Such modifications emerge from a functional connectivity analysis of EEG signals based on the graph theory.[16] This mathematical approach evaluates the properties of connections (edges) between pairs of brain areas (nodes). Several approaches are available to create a brain network model. More specifically, nodes could be the cortical sources of each EEG band signal (localized on the different Brodmann areas [BAs]) or the EEG scalp electrodes, while edges express a direct or indirect interaction between nodes, measured as a dichotomic unweighted variable (presence/absence) or as a continuous weighted parameter (eg, Lagged Linear Coherence).[17,18] In our case, we adopted an undirected, weighted brain network model where nodes were BAs and edges were the synchronization expressed as Lagged Linear Coherence. The graph theory-based analysis well describes local specialization and global integration of the brain networks. Local specialization describes a condition where nodes are highly connected within small groups and is measured by the clustering coefficient (*C*w).[19,20] On the other hand, global integration depends on the strength of connections between each node and all the other nodes of the network; a measure of global integration is the average shortest path length (*L*w).[19,20] If compared to mathematical graphs, whose global integration decreases when the number of nodes increases, brain networks tend to have a peculiar behavior.[21] In particular, brain networks maintain a balance between local specialization and global integration, being the latter preserved even when the network complexity increases: this peculiar network balance is called "small-worldness" (*S*w) and it is characterized by high functional segregation (high *C*w) and functional integration (low *L*w). Acute stroke influences such balance between local specialization and global integration, perturbing brain networks in a frequency-dependent way.[15,21,22] Moreover, our previous research showed that these changes are not influenced by size or side of the affected area.[15,23] Specifically, we found that acute brain damage caused by ischemic stroke induces a change in delta brain network architecture, compared to healthy sex- and age-matched subjects. In fact, on one hand it is associated with an increase of the strength of connections between functionally close BAs meaning an increase in local specialization (high *C*w); on the other hand, following stroke each node is more weakly connected with all the other nodes within the delta network meaning a decrease of global integration between BAs (high *L*w). We noticed a similar behavior for theta networks, but only in case of left hemispheric stroke. Considering that stroke usually induces a shift toward low-frequency EEG patterns[24,25] we can interpret such delta and theta network modifications as an attempt of the brain to confine the strong delta activity in clusters that are locally richly interconnected, but poorly integrated at global level. Regarding EEG high frequencies,

[1]Department of Emergency, Anaesthesiology and Intensive Care Medicine, Fondazione Policlinico Universitario A. Gemelli IRCCS, Rome, Italy[AQ: 1]
[2]Fondazione Policlinico Universitario A. Gemelli IRCCS, UOC Neuroriabilitazione ad Alta Intensità Largo Agostino Gemelli 8, Rome, Italy
[3]Department of Electrical and Electronic Engineering (DIEE), University of Cagliari, Cagliari, Italy
[4]UOC Neurologia, Dipartimento Neuroscienze, Organi di Senso, Torace, Fondazione Policlinico Universitario A. Gemelli IRCCS, Rome, Italy
[5]Department of Neuroscience, Catholic University of the Sacred Hearth, Rome, Italy
[6]Clinical Unit of Neurology, Department of Medicine, Surgery and Health Sciences, Trieste University Hospital, University of Trieste, Trieste, Italy
[7]Università degli Studi di Genova, IRCCS Ospedale Policlinico San Martino, Genova, Italy
[8]Department of Applied Clinical Sciences and Biotechnology, University of L'Aquila, L'Aquila, Italy
[9]Department of Geriatrics and Orthopaedics, Università Cattolica del Sacro Cuore, Rome, Italy
[10]UOS Riabilitazione Post-Acuzie, Fondazione Policlinico Universitario A. Gemelli IRCCS, Rome, Italy
[11]Department of Neuroscience, Division of Clinical Neurophysiology, IRCCS Ospedale Policlinico San Martino, Genova, Italy
[12]Department of Neuroscience, Rehabilitation, Ophthalmology, Genetics, Maternal and Child Health, University of Genoa, Genova, Italy

*These authors contributed equally to this work.

Supplementary material for this article is available on the *Neurorehabilitation & Neural Repair* website along with the online version of this article.

Corresponding Author:
Silvia Giovannini, Department of Geriatrics and Orthopaedics, Università Cattolica del Sacro Cuore, Fondazione Policlinico Universitario A. Gemelli IRCCS, Largo A. Gemelli, 8, Rome 00168, Italy.
Email: silvia.giovannini@unicatt.it

related to dominating rhythm of the healthy brain, we found that stroke induces functional local uncoupling between BAs in alpha networks, that is lower *C*w, counterbalanced by an increase of global integration, that is lower *L*w, as an effort to preserve the global effect of alpha rhythms throughout the brain. It is noteworthy that we found these brain network changes not only in the affected hemisphere but also in the opposite hemisphere and throughout the entire brain. The imbalance of the aforementioned specific network parameters resulted in *S*w modifications, with a global reduction of *S*w in low frequencies and a specular increase of *S*w in high frequencies.[15] These dynamic changes in brain connectivity embody the brain's effort to achieve a balance between the damage caused by the stroke and its compensatory reaction. This sort of *S*w network "homeostasis" has a two-fold impact: on one hand, it restricts the functional coupling between BAs that are clustered in "pathological" low-frequency networks, reducing their overall integration, while on the other hand it counteracts the impairment of "healthy" alpha clusters by enhancing their physiological global integration.[26]

Some studies investigated the interconnections between brain EEG-network *S*w and stroke symptoms and recovery.[27-30] One study found a prognostic value of delta and gamma *S*w after a rehabilitation period in post-stroke patients.[27] Exploring the relationship between anatomical lesions and brain connectivity, the authors of another study found that the degree of functional recovery after stroke is associated with the integrity degree of ipsilesional corticospinal tracts in combination with interhemispheric resynchronization and normalization of *S*w cortical network organization.[28] Regarding long-term stroke complications, 1 study found an association between *S*w rearrangements and risk of developing post-stroke cognitive impairment.[29] About the relationship between stroke severity and brain networks, 1 study found an association between low *S*w (delta, theta, alpha, and beta) and consciousness disorders in patients with acute/subacute stroke.[30]

We hypothesize that an early analysis of EEG-based resting state connectivity rearrangements in the hyperacute phase (within the first 24 hours following stroke onset) could provide critical information for formulating a more timely and reliable prognosis on clinical severity within the subacute phase.[31,32] The aim of this study is: (a) to identify topological network characteristics that are related with clinical severity in the hyperacute phase and at the end of the acute phase; (b) to identify topological network characteristics underlying the hyperacute phase that predict clinical severity in the acute/sub-acute phase (within 10 days).

Methods

A multicenter prospective observational study was conducted recruiting 87 patients (38 males and 49 females; age = 73 ± 13 years) with acute anterior circulation ischemic stroke (47% with a left hemispheric stroke). Patients were recruited in 4 different clinical centers in Italy (University Hospital Foundation A. Gemelli in Rome, University Hospital of Trieste, Hospital San Martino in Genoa, and University Hospital of L'Aquila).

According to recently proposed standardized definitions in stroke recovery research,[31,32] the hyperacute phase refers to the first 24 hours after stroke onset, the acute phase extends from day 1 to day 7, the early subacute phase from day 7 to 3 months, the late subacute phase from 3 to 6 months, and the chronic phase begins after 6 months. All patients were enrolled during stroke hyper-acute phase[31,32] and followed-up for the acute/sub-acute phase.[31,32] For clinical severity assessment, we used the National Institutes of Health Stroke Scale (NIHSS) within 24 hours from stroke onset (NIHSS at *T*0) and at discharge from sub-intensive stroke unit (NIHSS at *T*1, within 10 days from stroke onset). Median NIHSS at *T*0 was 10 (interquartile range [IQR] = 6-15), while the median NIHSS at *T*1 was 5 (IQR = 2-12). Table 1 shows the demographical and clinical characteristics of the recruited patients. All patients completed the study. EEG recordings were not optimal in 3 patients at *T*0 and in 6 patients at *T*1 and those recordings were excluded from the analysis.

Approval for the research was obtained from the local ethics committee (Fondazione Policlinico Universitario A. Gemelli IRCCS, Protocol Number 0007987/17) in accordance with the Helsinki Declaration. Each participant provided informed written consent.

Table 1. Demographical and Clinical Characteristics of Enrolled Stroke Patients.

Population characteristics (N = 87)	
Female (%)	57
Age (Median value, [IQR])	74 [65-84]
Atrial fibrillation (%)	32
Diabetes (%)	14
Hypertension (%)	79
Smoke (%)	21
Left hemispheric stroke (%)	47
Subcortical lesion (%)	35
Cortical lesion (%)	14
Cortical and subcortical lesion (%)	51
NIHSST_0 (Median value, [IQR])	10 [6-15]
NIHSST_1 (Median value, [IQR])	5 [2-12]
Cardioembolic etiology (%)	34
Atherosclerotic etiology (%)	18
Lacunar etiology (%)	16
Other etiology (%)	7
Unknown etiology (%)	25

Note. NIHSST_0 = NIHSS within 24 hours, NIHSST_1 = median day 6.

The inclusion criteria were: hemiparesis/hemiplegia, ischemic stroke in the middle cerebral artery territory regardless of the side, location, and size of the lesion. The exclusion criteria were: severe aphasia with inability to understand instructions for EEG recordings, disorder of consciousness (coma/unresponsive wakefulness syndrome), previous stroke (ischemic or hemorrhagic), diagnosis of epilepsy, previous cognitive impairment, or neurodegenerative disorder.

EEG recordings were performed by BRAIN QUICK® LTM—SD LTM PLUS 32 (Micromed S.p.A, Italy) for at least 20 minutes while patients had their eyes closed, in a resting state, respectively within 24 hours after stroke onset (*T*0) and within 10 days (*T*1).[33,34] EEG signals were acquired by 31 brain electrodes placed following the 10-10 system, with a common reference electrode placed on the mastoid and a ground electrode. We decided not to use a larger number of electrodes to make the recording process easier, since it was undertaken in the complex environment of a sub-intensive care unit. Moreover, the number of electrodes is enough to have an insight on brain network since we were operating in the context of low-resolution brain electromagnetic tomography.[35,36] We monitored EEG activity in order to identify specific paroxysmal sleep-related activities and exclude recordings in case patients were falling asleep. EEG data were continuously recorded during the 2 sessions at a sampling rate of 512 Hz.

EEG Data Analysis

EEG data underwent preprocessing in Matlab R2018 (Math-Works Inc, Natick, MA, USA) using EEGLAB 12 (http://www.sccn.ucsd.edu/eeglab). To eliminate muscle artifacts, the EEG recordings underwent band-pass filtering between 1 and 30 Hz, as muscular contraction typically exhibits frequencies higher than 30 Hz.[37] Independent component analysis (ICA),[38] along with the RELICA algorithm,[39] were used to remove visible artifacts such as eye movements, cardiac activity, and scalp muscle contraction. The non-brain signals were excluded from the subsequent analysis using an index retention threshold of 85%.

Functional Brain Connectivity

In order to assess the resting-state functional connectivity of the brain, we processed EEG data using sLORETA (low-resolution brain electromagnetic tomography; http://www.uzh.ch/keyinst/NewLORETA/LORETA01.htm).[35] This software helped us locate the cortical sources of brain activity. The EEG cross-spectra and the 3D-cortical distribution of the electric neuronal generators were computed for each frequency band considered in the study (ie, delta: 1-4 Hz, theta: 4-8 Hz, alpha1: 8-11 Hz, and alpha2: 11-13 Hz) in both *T*0 and *T*1 evaluations, separately for each subject.[36,40] We excluded gamma and beta frequency bands from the analysis of resting-state network rearrangements based on previous evidence[15,25,41] indicating a lack of consistent reorganization in these bands under resting conditions. This decision is further supported by the hypothesis that coherence in faster rhythms, such as beta and gamma, is more relevant to active processes, including motor or cognitive tasks, rather than resting-state activity.[42-44] The solution space was restricted to the cortical gray matter, as defined by the probabilistic Talairach atlas[45] and the Montreal Neurologic Institute average MRI brain was used as a realistic head model.[46]

To analyze the functional brain connectivity, we used lagged linear coherence (LLC) at the source space. LLC excludes coherences with zero phase lag,[47] and it is not affected by volume conduction. For this analysis, we used a whole-brain BAs atlas to select the 42 BAs in each hemisphere as region of interest (ROI). This allowed us to perform the functional brain connectivity analysis between pairs of ROIs for each time of evaluation (*T*0 and *T*1).

LLC in a specific frequency band ω is defined by the following equation:

$$\rho^2{}_{xy}(\omega) = \frac{[\mathrm{Im}(s_{xy}(\omega))]^2}{s_{xx}(\omega)s_{yy}(\omega) - [\mathrm{Re}(s_{xy}(\omega))]^2}$$

Where s_{xx} and s_{yy} are the power spectral densities of 2 source signals *x* and *y* respectively, s_{xy} is the cross power spectral density of *x* and *y*, and ω is the reference frequency band.[47]

Connectivity parameters between all pairs of ROIs for each frequency band and for each subject were used a measure of weight of the graph in the graph analyses.[48]

Graph Analysis

Using the Brain Connectivity Toolbox (https://sites.google.com/site/bctnet/), we computed several network metrics, often referred to as topological network characteristics, to summarize the global architecture for each weighted connection matrix. The segregation of the network was measured by the mean weighted clustering coefficient (*C*w), while the integration was assessed by the mean weighted characteristic path length (*L*w). *C*w was obtained by averaging the weighted clustering coefficient of each individual node in the network, while *L*w represents the average of the shortest weighted paths connecting each node to all the other nodes.[49,50] To account for variations across subjects, the values of *C*w and *L*w for each frequency band (δ, θ, α1, α2, and β) were normalized using the global mean value obtained by averaging these parameters across all 5 bands.

To estimate the functional integration of the network, we computed the *S*w coefficient as a ratio between *C*w and *L*w normalized to the Cw_{rand} and Lw_{rand} of an equivalent weighted random network[49,50] respectively, as described by the following equation:

$$Sw = \frac{Cw / Cw_{rand}}{Lw / Lw_{rand}}$$

The *S*w coefficient measures the balance between the local connectedness and the global integration of a network and it is calculated for each subject. This is a scaled measure indicating the *S*w property of the network when the ratio is higher than 1. In such case, *L*w is similar to that of a random equivalent graph and/or the network's *C*w is larger than that of the equivalent random graph.

Statistical Analysis

All statistical analyses were performed in Statistical Package for the Social Sciences statistics software (version 20.0, IBM Corp., Armonk, NY, USA). The Shapiro–Wilk probability test was used to assess the normality of the distributions. Accordingly, the Wilcoxon non-parametric test was used to compare the medians of each connectivity parameter (*C*w, *L*w, and *S*w) between *T*0 and *T*1. The Pearson's test was used to correlate each graph parameter (*C*w, *L*w, and *S*w) measured at *T*0 with the corresponding NIHSS score at *T*0. The same approach was applied for *T*1 data.

Moreover, in order to investigate the impact of connectivity parameters as a whole on the clinical severity, a multiple linear regression model with the stepwise method was used. We built 3 regression models: in the first, NIHSS at *T*0 was the dependent variable and *C*w, *L*w, and *S*w obtained at *T*0 for each frequency band were the independent variables; in the second, NIHSS at *T*1 was the dependent variable and *C*w, *L*w, and *S*w obtained at *T*1 were the independent variables; in the last, NIHSS at *T*1 was the dependent variable and *C*w, *L*w, and *S*w obtained at *T*0 were the independent variables. *P*-value significance was set at .05.

Population Characteristics

We enrolled 87 consecutive patients (57% female, median age = 75 years), 47% having a left hemispheric stroke. The median NIHSS at *T*0 was 10 (IQR = 6-15), while the median NIHSS at *T*1 was 5.5 (IQR = 2-12). The overall hospitalization had a median duration of 6 days (range = 4–10 days). The clinical severity, expressed as NIHSS total score, was found to be statistically higher at *T*0 than at *T*1 (Wilcoxon, $P < .001$). Table 1 shows the demographical and clinical characteristics of the recruited patients.

Results

Supplemental materials show the variation of each topological parameter between *T*0 and *T*1. Briefly, we found higher integration (decrease of *L*w) and higher global efficiency (increase of *S*w) in alpha band at *T*1.

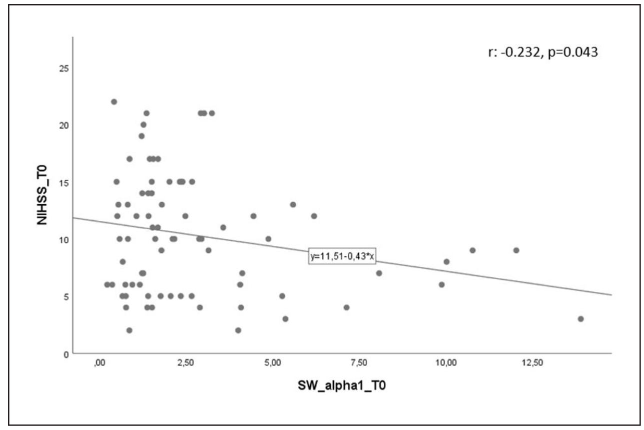

Figure 1. Negative correlation between alpha1 *S*w and NIHSS at admission (*T*0).

Correlations Between Connectivity Parameters and Clinical Severity

At *T*0 we found a statistically significant negative correlation between alpha1 *S*w and NIHSS ($r = -.232$, $P = .043$; Figure 1), meaning that more severe symptoms are associated with a greater impairment of network balance between local specialization and global integration in the alpha frequencies. We found no statistically significant correlations between other connectivity parameters at *T*0 and NIHSS at *T*0.

At *T*1, NIHSS correlates with delta *S*w ($r = .423$, $P = .0001$), delta *C*w ($r = .346$, $P = .003$), and delta *L*w ($r = -.366$, $P = .002$; Figure 2). These results imply that more severe symptoms are associated to an increase of local specialization and an increase of global integration in slow delta frequencies, resulting in a shift of delta *S*w toward higher values. Moreover, NIHSS at *T*1 correlates with alpha1 *C*w ($r = -.280$, $P = .017$) and alpha1 *L*w ($r = .359$, $P = .002$; Figure 3). These results mean that more severe symptoms are associated with a reduction of local specialization and a decrease of global integration in alpha frequencies.

Connectivity Parameters and Stroke Severity: Linear Regression

Using NIHSS as dependent variable and connectivity parameters for each frequency band as independent variables, we obtained models to explore the relationship between brain networks at *T*0 and clinical severity at *T*0, between brain networks at *T*1 and clinical severity at *T*1 and, finally, between brain networks at *T*0 and clinical severity at *T*1.

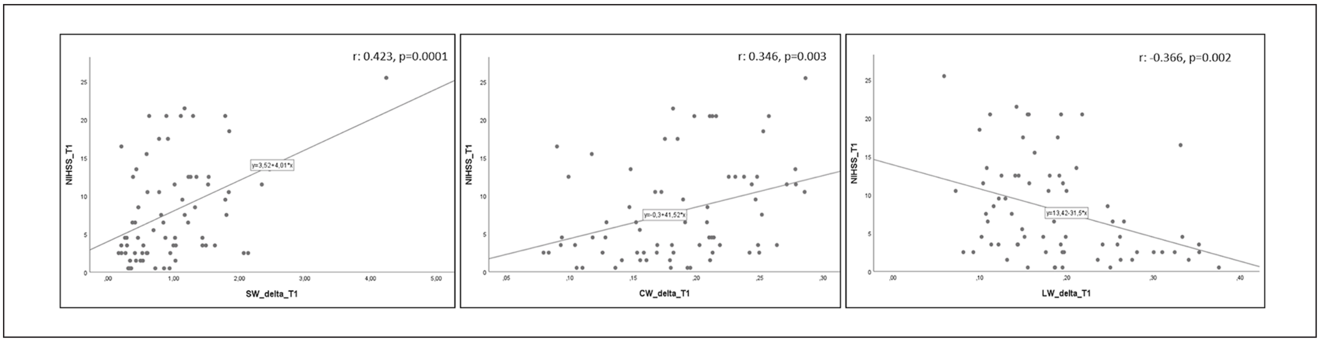

Figure 2. Correlation plot between low frequency network connectivity parameters at discharge and NIHSS at discharge (*T*1). On the left, positive correlation between delta *S*w and NIHSS *T*1; in the center positive correlation between delta *C*w and NIHSS at *T*1; on the right, negative correlation between delta Lw and NIHSS at *T*1.

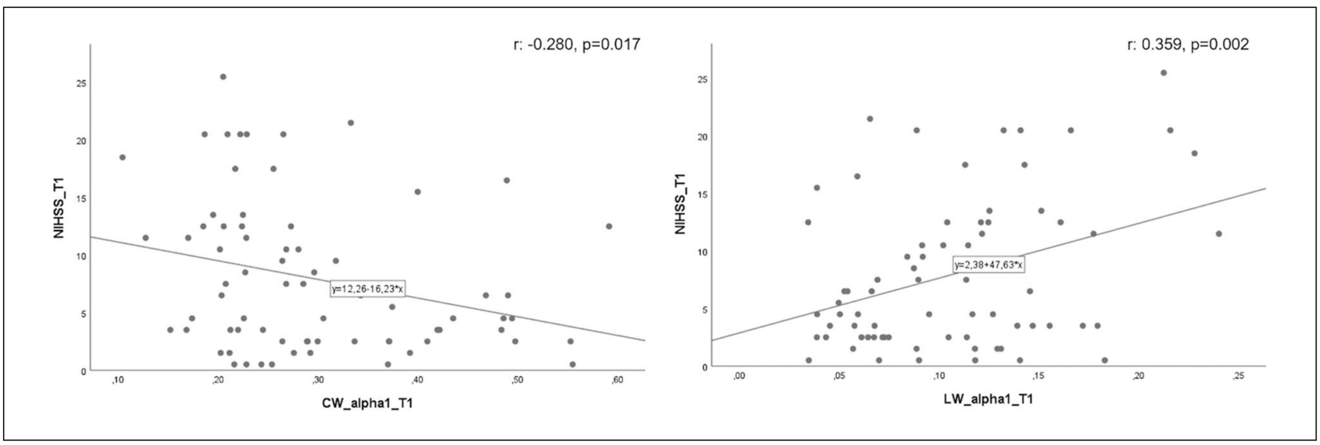

Figure 3. Correlation plot between alpha network connectivity parameters at discharge and NIHSS at discharge (*T*1). On the left negative correlation between alpha1 *C*w and NIHSS at *T*1; on the right, positive correlation between alpha1 *L*w and NIHSS at *T*1.

In the first model ($F=4.255$, $P=.04$) we found a negative association between alpha1 *S*w at *T*0 and global NIHSS at *T*0 ($\beta=-.232$, $P=.04$). In the second model ($F=15.223$, $P<.001$), we found a positive association between delta *S*w and global NIHSS at *T*1 ($\beta=.423$, $P<.001$). Finally, in the third model ($F=5.324$, $P=.02$), we found a positive association between delta *S*w at *T*0 and NIHSS at *T*1 ($\beta=.259$, $P=.02$).

Discussion

Our findings not only strengthen previous evidence, pointing out that network rearrangements after stroke follow a frequency-dependent modality,[15,23,51] but also suggest that specific network changes within 24 hours, in particular *S*w and *C*w in delta band, can predict stroke severity at discharge. This aligns with a growing body of literature that employs resting-state EEG to identify biomarkers of stroke recovery. For example, Saes et al[12,13] demonstrated that early EEG spectral characteristics, such as Brain Symmetry Index in the theta band, can predict upper limb motor impairment months after stroke, highlighting the prognostic potential of EEG measures recorded in the first phase.[12,13] While these studies focused primarily on spectral power and symmetry, with EEG typically performed within the first 3 weeks post-stroke, our work extends this approach by investigating the topological properties of brain networks, offering a complementary perspective on EEG-derived biomarkers and anticipating the timing of EEG acquisition (targeting in the hyperacute phase: into the first 24 hours after stroke onset) according to the timeline defined by Bernhardt et al.[31,32] Similarly, in chronic stroke, Zhang et al[14] found correlations between resting-state EEG rhythms, network metrics (like node strength in the delta band), and motor function, emphasizing the lasting impact of network alterations.

In this study, we found that an increased *S*w of delta network and a high segregation (*C*w) of delta frequencies at admission are associated with severe stroke symptoms at discharge. Such increase of delta network rearrangement might depend on the increase of the local strength of delta connections between BAs induced by the ischemic lesion itself. In fact, stroke induces an EEG shift to a low frequency pattern,[24,25] with subsequent delta network rearrangement in both hemispheres, with increased clustering (*C*w) and increased path length (*L*w).[15] This is probably an attempt to counterbalance the effect of stroke, confining pathologically clustered BAs and reducing their global interconnection.[26] Indeed, we know that neuronal slow oscillations, an alternation of firing and silence at the frequency of 1 Hz, are the neurophysiological correlate of default mode network and are prominent during slow-wave sleep, anesthesia, and brain injury, including stroke.[52] A potential neurophysiological basis of the network architecture reorganization we observed in slow rhythms might depend on the cortical bistability phenomenon, that is the tendency of cortical areas to stay in a hyperpolarized, unexcitable state, which prevents global spreading of noninvasive magnetic stimulation inducing only local network activation because of the unexcitable state of the nearest areas.[52,53] Further studies with a combination of transcranial magnetic stimulation and EEG-based network analysis might give a deeper insight into such large- and small-scale interconnections. This might be achieved by evaluating the relationship between the perturbational complexity index, that evaluates the spread of network response to a brain stimulus, and measures of global integration and local segregation of the network. It is reasonable to hypothesize that stroke patients with lower global integration might exhibit a little spread of brain response to a TMS stimulus. Although the associations between network topology measures (eg, delta-band *S*w at admission) and clinical severity (NIHSS at discharge), the effect sizes were modest, indicating that each individual network metric accounts for a limited portion of outcome variance. However, demonstrating the association between definitive set of EEG measures and clinical outcome is of primary importance because the integration of such metrics within a more comprehensive and multimodal model could contribute to increase the accuracy of prognostication. EEG-based measures capture functional brain activity and offer complementary information to clinical and structural imaging data. For example, Vanderschelden et al[54] reported that adding a spectral EEG biomarker to standard predictors (eg, age, diabetes status, and infarct volume) increased explained variance in initial NIHSS from 47% to 60%. Moreover, EEG functional measures can enhance prognostic accuracy beyond prediction afforded by standard clinical assessments.[55] as well as an integrated model, combining EEG assessment of brain network and indicators of anatomical neural injury, outperforms radiological findings in capturing clinical severity after stroke.[56] In our study, topological measures such as *S*w, *C*w, and *L*w provide a complementary perspective on how stroke disrupts global and local brain network efficiency. While individually limited, their integration into multimodal models might enhance prognostic accuracy and guide targeted neurorehabilitation.

Regarding high frequencies, we know that, compared to healthy individuals, acute ischemic stroke patients present modifications of the alpha network, which relates with the dominating rhythm of the healthy brain.[15,23,57] Our findings suggest that alpha network homeostatic response is somehow correlated to clinical severity. More deeply, from correlation analysis, we found that high segregation and high integration (respectively, high *C*w and low *L*w) of alpha 1 networks are associated with less severe symptoms at discharge (Figure 3). The importance of alpha1 network response to ischemic damage is even more relevant if we consider the results of the regression analysis, which shows that the higher is the alpha1-*S*w at admission, the lower is the NIHSS at admission.

Evaluating stroke-induced network rearrangement in the very early phase of stroke and observing its evolution is crucial to understand the effects of the ischemic lesion on the brain functioning. In a subgroup analysis of the WAKE-UP trial, a functional MRI analysis showed that brain networks tend to increase their segregation and decrease their integration after 36 hours, especially in patients with poor functional outcome.[58] Here, we conducted a similar analysis, being able to study such network reorganization in a frequency-dependent modality, thanks to the use of EEG-based analysis. We found that some of the network features obtained in the first 24 hours, such as delta network segregation (*C*w), remain steadily associated to severe stroke symptoms until discharge. Moreover, and interestingly, we found further delta network rearrangements in the following days, observing that increased delta global integration (reduced *L*w) at discharge is associated with more severe stroke symptoms at discharge. This is probably due to a specific brain network 'homeostatic' response that starts soon after the ischemic damage and continues in the following days.[26] Looking at correlation and regression analysis, we were able to identify those topological parameters that are suggestive of homeostatic failure or homeostatic success, in other words a network rearrangement associated with more or less severe neurological symptoms.

Our study highlights how resting-state EEG complements and expands upon previous findings primarily obtained through fMRI in stroke.[59,60] While fMRI has demonstrated impaired integration and segregation in resting-state networks during the acute and subacute phase of stroke, EEG adds a dynamic layer of information by directly capturing the oscillatory activity of neuronal assemblies with high temporal resolution. This allows for the identification of frequency-specific network changes that reflect both pathological and compensatory mechanisms, as also suggested by studies focusing on EEG power spectra and symmetry in relation to clinical recovery.[12,13] Unlike imaging techniques such as fMRI, which focus on slower hemodynamic responses, EEG captures neural activity with millisecond-level temporal resolution. This is particularly important in the context of acute stroke, where rapid changes in brain dynamics can occur. Additionally, EEG's ability to analyze specific frequency bands allows us to investigate how different rhythms contribute to cortical network rearrangements, offering valuable insight into both pathological disruptions and compensatory processes. These features, together with the bed-side feasibility, make EEG an ideal tool for exploring early functional connectivity changes that might predict clinical outcomes at discharge. The broader utility of EEG in stroke prognostication is well-supported by the systematic review by Vatinno et al,[55] which confirmed significant associations between various EEG measures and key clinical outcomes (Modified Rankin Score [mRS], NIHSS, and Fugl-Meyer Upper Extremity).[55] Our work contributes to this by specifically identifying early EEG-based network topological features (EEG performed during hyperacute phase after index event) as potentially valuable components in this prognostic toolkit.

Finally, some limitations of our study deserve comment. First, in this study we explored the relationship between network characteristics within 24 hours of stroke onset and evolution of clinical severity within the acute/subacute phase.[31,32] However, NIHSS at discharge from the hospital is a good surrogate outcome of mRS at 3 months.[61] In this view, topological features of network rearrangement within 24 hours could be informative on long term clinical evolution although further investigations are needed to confirm it. Furthermore, although NIHSS at stroke onset is the most important prognostic factor in stroke patients,[62] prognostic accuracy of experienced clinicians is still low, even in patients with low NIHSS.[63] Moreover, even advanced artificial intelligence models do not have a full accuracy in predicting stroke evolution.[64] Probably, we need an integrated, multi-layer model to effectively describe the multi-faceted and complex mechanisms of stroke recovery. These models should be based not only on the variables available from daily clinical practice, such as demographic, clinical, and radiological data, but also on innovative biomarkers and neurophysiological variables. In this view, although the association between network topological modifications and clinical severity might not seem strong enough to predict stroke recovery alone, we provide a neurophysiological biomarker to be tested in further multi-dimensional prognostic models. Such integration might contribute to enhance the predictive performance considering the interrelationship between variables belonging to different domains.

Another limitation is probably linked to the overall improvement of all patients during our observation (median final NIHSS 5.5 vs initial 10). This might have limited our ability to identify specific network signatures associated with neurological deterioration.

Conclusions

In conclusion, our findings show that, in patients with ischemic stroke, early rearrangement patterns of delta network small-worldness have a potential prognostic role for predicting clinical severity at the end of the acute phase. In this view, integrating network properties in a prognostic model together with other clinical variables needs to be further explored.

Future research should also investigate the influence of lesion location on this relationship as well as the potential role of spectral characteristics as a prognostic biomarker of recovery. Although EEG analysis requires methodological rigor and specialized expertise, its portability, repeatability, and direct neurophysiological relevance make it a promising adjunct to clinical scales. Future work should focus on integrating EEG metrics into composite prediction models and exploring their responsiveness to targeted neurorehabilitation interventions.

Acknowledgments

None.

List of Abbreviations and Definitions

$T0$: first observation, within 24 hours from stroke onset
$T1$: second observation, within 10 days from stroke onset
Cw: weighted clustering coefficient, a measure of local segregation in network analysis
Lw: weighted average shortest path length, a measure of global integration in network analysis
Sw: the ratio between Cw and Lw, it is a measure of the balance between local segregation and global integration. The higher it is, the higher is the network efficiency
BAs: Brodmann areas
LLC: lagged linear coherence, a measure of functional synchronization in EEG analysis

Author Contributions

Chiara Iacovelli: Conceptualization; Data curation; Project administration; Software; Validation; Writing—original draft; and Writing—review & editing. Giuseppe Reale: Conceptualization; Formal analysis; Investigation; Project administration; Resources; Supervision; Writing—original draft; and Writing—review & editing. Giulia Baldazzi: Formal analysis; Supervision; and Writing—review & editing. Danilo Pani: Investigation; Methodology; Validation; and Writing—review & editing. Aurelia Zauli: Conceptualization; Data curation; Resources; Visualization; and Writing—review & editing. Marco Moci: Conceptualization; Formal analysis; Investigation; Resources; and Writing—review & editing. Paolo Manganotti: Funding acquisition; Investigation; Supervision; and Writing—review & editing. Lucio Marinelli:

Formal analysis; Supervision; Visualization; and Writing—review & editing. Simona Sacco: Methodology; Project administration; Validation; and Writing—review & editing. Giovanni Furlanis: Data curation; Funding acquisition; Visualization; and Writing—review & editing. Miloš Ajčević: Data curation; Methodology; Resources; and Writing—review & editing. Silvia Giovannini: Conceptualization; Data curation; Funding acquisition; and Writing—review & editing. Simona Crosetti: Formal analysis; Funding acquisition; Resources; Software; and Writing—review & editing. Matteo Grazzini: Data curation; Methodology; Software; Validation; and Writing—review & editing. Marta Garbuglia: Formal analysis; Visualization; and Writing—review & editing. Pietro Caliandro: Conceptualization; Data curation; Formal analysis; Methodology; Project administration; Supervision; and Writing—original draft.

Declaration of Conflicting Interests

The author(s) declared no potential conflicts of interest with respect to the research, authorship, and/or publication of this article.

Funding

The author(s) received no financial support for the research, authorship, and/or publication of this article.

ORCID iDs

Lucio Marinelli https://orcid.org/0000-0003-0620-7654
Silvia Giovannini https://orcid.org/0000-0001-9125-752X
Pietro Caliandro https://orcid.org/0000-0002-1190-4879

References

1. Cassidy JM, Mark JI, Cramer SC. Functional connectivity drives stroke recovery: shifting the paradigm from correlation to causation. *Brain*. 2022;145:1211-1228.
2. Karnadipa T, Chong B, Shim V, Fernandez J, Lin DJ, Wang A. Mapping stroke outcomes: a review of brain connectivity atlases. *J Neuroimaging*. 2024;34:548-561.
3. Tang C-W, Hsiao F-J, Lee P-L, et al. β-oscillations reflect recovery of the paretic upper limb in subacute stroke. *Neurorehabil Neural Repair*. 2020;34:450-462.
4. Bönstrup M, Krawinkel L, Schulz R, et al. Low-frequency brain oscillations track motor recovery in human stroke. *Ann Neurol*. 2019;86:853-865.
5. Ramanathan DS, Guo L, Gulati T, et al. Low-frequency cortical activity is a neuromodulatory target that tracks recovery after stroke. *Nat Med*. 2018;24:1257-1267.
6. Hoshino T, Oguchi K, Inoue K, Hoshino A, Hoshiyama M. Relationship between upper limb function and functional neural connectivity among motor related-areas during recovery stage after stroke. *Top Stroke Rehabil*. 2020;27:57-66.
7. Park C, Chang WH, Ohn SH, et al. Longitudinal changes of resting-state functional connectivity during motor recovery after stroke. *Stroke*. 2011;42:1357-1362.
8. Lee J, Park E, Lee A, Chang WH, Kim D-S, Kim Y-H. Alteration and role of interhemispheric and intrahemispheric connectivity in motor network after stroke. *Brain Topogr*. 2018;31:708-719.
9. Wang L, Yu C, Chen H, et al. Dynamic functional reorganization of the motor execution network after stroke. *Brain*. 2010;133:1224-1238.
10. Golestani A-M, Tymchuk S, Demchuk A, Goodyear BG, VISION-2 Study Group. Longitudinal evaluation of resting-state FMRI after acute stroke with hemiparesis. *Neurorehabil Neural Repair*. 2013;27:153-163.
11. Rehme AK, Eickhoff SB, Wang LE, Fink GR, Grefkes C. Dynamic causal modeling of cortical activity from the acute to the chronic stage after stroke. *Neuroimage*. 2011;55:1147-1158.
12. Saes M, Zandvliet SB, Andringa AS, et al. Is resting-state EEG longitudinally associated with recovery of clinical neurological impairments early poststroke? A prospective cohort study. *Neurorehabil Neural Repair*. 2020;34:389-402.
13. Saes M, Meskers CGM, Daffertshofer A, Van Wegen EEH, Kwakkel G. Are early measured resting-state EEG parameters predictive for upper limb motor impairment six months post-stroke? *Clin Neurophysiol*. 2021;132:56-62.
14. Zhang JJ, Bai Z, Fong KNK. Resting-state cortical electroencephalogram rhythms and network in patients after chronic stroke. *J NeuroEng Rehabil*. 2024;21:32.
15. Caliandro P, Vecchio F, Miraglia F, et al. Small-world characteristics of cortical connectivity changes in acute stroke. *Neurorehabil Neural Repair*. 2017;31:81-94.
16. Boccaletti S, Pecora LM. Introduction: stability and pattern formation in networks of dynamical systems. *Chaos*. 2006;16:015101.
17. Friston KJ. Functional and effective connectivity: a review. *Brain Connect*. 2011;1:13-36.
18. Friston KJ, Worsley KJ, Frackowiak RS, Mazziotta JC, Evans AC. Assessing the significance of focal activations using their spatial extent. *Hum Brain Mapp*. 1994;1:210-220.
19. Stam CJ, Reijneveld JC. Graph theoretical analysis of complex networks in the brain. *Nonlinear Biomed Phys*. 2007;1:3.
20. Bassett DS, Bullmore E. Small-world brain networks. *Neuroscientist*. 2006;12:512-523.
21. Watts DJ, Strogatz SH. Collective dynamics of "small-world" networks. *Nature*. 1998;393:440-442.
22. Tononi G. Reentry and the problem of cortical integration. *Int Rev Neurobiol*. 1994;37:127-152; discussion 203-207.
23. Vecchio F, Miraglia F, Rossini PM. Tracking neuronal connectivity from electric brain signals to predict performance. *Neuroscientist*. 2019;25:86-93.
24. Wang L, Guo X, Sun J, Jin Z, Tong S. Cortical networks of hemianopia stroke patients: a graph theoretical analysis of EEG signals at resting state. *Annu Int Conf IEEE Eng Med Biol Soc*. 2012;2012:49-52.
25. Dubovik S, Pignat J-M, Ptak R, et al. The behavioral significance of coherent resting-state oscillations after stroke. *Neuroimage*. 2012;61:249-257.
26. Caliandro P, Reale G, Vecchio F, et al. Defining a functional network homeostasis after stroke: EEG-based approach is complementary to functional MRI. *Brain*. 2017;140:e71.
27. Vecchio F, Tomino C, Miraglia F, et al. Cortical connectivity from EEG data in acute stroke: a study via graph theory as a potential biomarker for functional recovery. *Int J Psychophysiol*. 2019;146:133-138.

28. van Meer MPA, Otte WM, van der Marel K, et al. Extent of bilateral neuronal network reorganization and functional recovery in relation to stroke severity. *J Neurosci*. 2012;32:4495-4507.
29. Costa C, Vecchio F, Romoli M, et al. Cognitive decline risk stratification in people with late-onset epilepsy of unknown etiology: an electroencephalographic connectivity and graph theory pilot study. *J Alzheimers Dis*. 2022;88:893-901.
30. Huang H, Niu Z, Liu G, et al. Early consciousness disorder in acute large hemispheric infarction: an analysis based on quantitative EEG and brain network characteristics. *Neurocrit Care*. 2020;33:376-388.
31. Bernhardt J, Borschmann K, Boyd L, et al. Moving rehabilitation research forward: developing consensus statements for rehabilitation and recovery research. *Neurorehabil Neural Repair*. 2017;31:694-698.
32. Bernhardt J, Hayward KS, Kwakkel G, et al. Agreed definitions and a shared vision for new standards in stroke recovery research: the stroke recovery and rehabilitation roundtable taskforce. *Int J Stroke*. 2017;12:444-450.
33. Krukow P, Rodríguez-González V, Kopiś-Posiej N, Gómez C, Poza J. Tracking EEG network dynamics through transitions between eyes-closed, eyes-open, and task states. *Sci Rep*. 2024;14:17442.
34. Tan B, Kong X, Yang P, Jin Z, Li L. The difference of brain functional connectivity between eyes-closed and eyes-open using graph theoretical analysis. *Comput Math Methods Med*. 2013;2013:1-15.
35. Pascual-Marqui RD. Standardized low-resolution brain electromagnetic tomography (sLORETA): technical details. *Methods Find Exp Clin Pharmacol*. 2002;24 Suppl D:5-12.
36. Pascual-Marqui RD, Michel CM, Lehmann D. Low resolution electromagnetic tomography: a new method for localizing electrical activity in the brain. *Int J Psychophysiol*. 1994;18:49-65.
37. Schomer DL. Ambulatory EEG monitoring, reviewing, and interpreting. *J Clin Neurophysiol*. 2021;38:77-86.
38. Hyvärinen A. Fast and robust fixed-point algorithms for independent component analysis. *IEEE Trans Neural Netw*. 1999;10:626-634.
39. Artoni F, Menicucci D, Delorme A, Makeig S, Micera S. RELICA: a method for estimating the reliability of independent components. *Neuroimage*. 2014;103:391-400.
40. Frei E, Gamma A, Pascual-Marqui R, Lehmann D, Hell D, Vollenweider FX. Localization of MDMA-induced brain activity in healthy volunteers using low resolution brain electromagnetic tomography (LORETA). *Hum Brain Mapp*. 2001;14:152-165.
41. Westlake KP, Hinkley LB, Bucci M, et al. Resting state α-band functional connectivity and recovery after stroke. *Exp Neurol*. 2012;237:160-169.
42. Gerloff C, Bushara K, Sailer A, et al. Multimodal imaging of brain reorganization in motor areas of the contralesional hemisphere of well recovered patients after capsular stroke. *Brain*. 2006;129:791-808.
43. de Vico Fallani F, Astolfi L, Cincotti F, et al. Evaluation of the brain network organization from EEG signals: a preliminary evidence in stroke patient. *Anat Rec*. 2009;292:2023-2031.
44. Jin S-H, Lin P, Hallett M. Reorganization of brain functional small-world networks during finger movements. *Hum Brain Mapp*. 2012;33:861-872.
45. Lancaster JL, Woldorff MG, Parsons LM, et al. Automated Talairach atlas labels for functional brain mapping. *Hum Brain Mapp*. 2000;10:120-131.
46. Mazziotta J, Toga A, Evans A, et al. A probabilistic atlas and reference system for the human brain: International Consortium for Brain Mapping (ICBM). *Philos Trans R Soc Lond B Biol Sci*. 2001;356:1293-1322.
47. Pascual-Marqui RD. Instantaneous and lagged measurements of linear and nonlinear dependence between groups of multivariate time series: frequency decomposition. 2007. Accessed February 27, 2025. http://arxiv.org/abs/0711.1455
48. Langer N, Pedroni A, Jäncke L. The problem of thresholding in small-world network analysis. *PLoS ONE*. 2013;8:e53199.
49. Rubinov M, Sporns O. Complex network measures of brain connectivity: uses and interpretations. *Neuroimage*. 2010;52:1059-1069.
50. Onnela J-P, Saramäki J, Kertész J, Kaski K. Intensity and coherence of motifs in weighted complex networks. *Phys Rev E Stat Nonlin Soft Matter Phys*. 2005;71:065103.
51. Vecchio F, Pappalettera C, Miraglia F, et al. Prognostic role of hemispherical functional connectivity in stroke: a study via graph theory versus coherence of electroencephalography rhythms. *Stroke*. 2023;54:499-508.
52. Sanchez-Vives MV, Massimini M, Mattia M. Shaping the default activity pattern of the cortical network. *Neuron*. 2017;94:993-1001.
53. Sarasso S, D'Ambrosio S, Fecchio M, et al. Local sleep-like cortical reactivity in the awake brain after focal injury. *Brain*. 2020;143:3672-3684.
54. Vanderschelden B, Erani F, Wu J, de Havenon A, Srinivasan R, Cramer SC. A measure of neural function provides unique insights into behavioral deficits in acute stroke. *Stroke*. 2023;54(2):e25-e29.
55. Vatinno AA, Simpson A, Ramakrishnan V, Bonilha HS, Bonilha L, Seo NJ. The prognostic utility of electroencephalography in stroke recovery: a systematic review and meta-analysis. *Neurorehabil Neural Repair*. 2022;36:255-268.
56. Wu J, Srinivasan R, Burke Quinlan E, Solodkin A, Small SL, Cramer SC. Utility of EEG measures of brain function in patients with acute stroke. *J Neurophysiol*. 2016;115:2399-2405.
57. Cantero JL, Atienza M, Salas RM, et al. Effects of prolonged waking-auditory stimulation on electroencephalogram synchronization and cortical coherence during subsequent slow-wave sleep. *J Neurosci*. 2002;22(11):4702-4708.
58. Schlemm E, Jensen M, Kuceyeski A, et al. Early effect of thrombolysis on structural brain network organisation after anterior-circulation stroke in the randomized WAKE-UP trial. *Hum Brain Mapp*. 2022;43:5053-5065.
59. Schlemm E, Ingwersen T, Königsberg A, et al. Preserved structural connectivity mediates the clinical effect of thrombolysis in patients with anterior-circulation stroke. *Nat Commun*. 2021;12:2590.
60. Adhikari MH, Hacker CD, Siegel JS, et al. Decreased integration and information capacity in stroke measured by

whole brain models of resting state activity. *Brain*. 2017;140: 1068-1085.

61. Chalos V, van der Ende NAM, Lingsma HF, et al. National Institutes of Health Stroke Scale: an alternative primary outcome measure for trials of acute treatment for ischemic stroke. *Stroke*. 2020;51:282-290.
62. Adams HP, Davis PH, Leira EC, et al. Baseline NIH Stroke Scale score strongly predicts outcome after stroke: a report of the Trial of Org 10172 in Acute Stroke Treatment (TOAST). *Neurology*. 1999;53:126-131.
63. Saposnik G, Cote R, Mamdani M, et al. JURaSSiC: accuracy of clinician vs risk score prediction of ischemic stroke outcomes. *Neurology*. 2013;81:448-455.
64. Caliandro P, Lenkowicz J, Reale G, et al. Artificial intelligence to predict individualized outcome of acute ischemic stroke patients: the SIBILLA project. *Eur Stroke J*. 2024;9:1053-1062.